

Drilling into the Metabolomics to Enhance Insight on Corn and Wheat Responses to Molybdenum Trioxide Nanoparticles

Xiangning Huang, Pabel Cervantes-Avilés, Weiwei Li, and Arturo A. Keller*



Cite This: <https://doi.org/10.1021/acs.est.1c00803>



Read Online

ACCESS |



Metrics & More



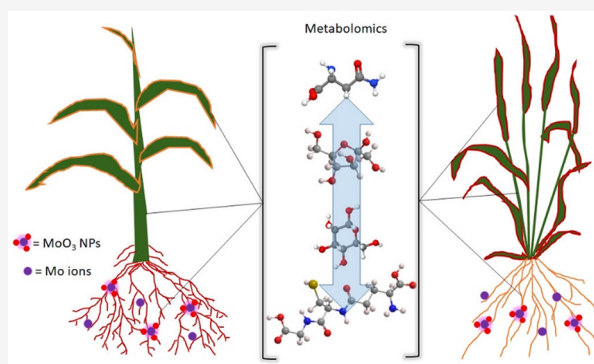
Article Recommendations



Supporting Information

ABSTRACT: Metabolomics is an emerging tool to understand the potential implications of nanotechnology, particularly for agriculture. Although molybdenum (Mo) is a known plant micronutrient, little is known of its metabolic perturbations. Here, corn and wheat seedlings were exposed to MoO_3 nanoparticles (NPs) and the corresponding bioavailable Mo^{6+} ion at moderate and excessive levels through root exposures. Physiologically, corn was more sensitive to Mo, which accumulated up to 3.63 times more Mo than wheat. In contrast, metabolomics indicated 21 dysregulated metabolites in corn leaves and 53 in wheat leaves. Five more metabolomic pathways were perturbed in wheat leaves compared to corn leaves. In addition to the overall metabolomics analysis, we also analyzed individual metabolite classes (e.g., amino acids, organic acids, etc.), yielding additional dysregulated metabolites in plant tissues: 7 for corn and 7 for wheat. Most of these were amino acids as well as some sugars. Additional significantly dysregulated metabolites (e.g., asparagine, fructose, reduced glutathione, mannose) were identified in both corn and wheat, due to Mo NP exposure, by employing individual metabolite group analysis. Targeted metabolite analysis of individual groups is thus important for finding additional significant metabolites. We demonstrate the value of metabolomics to study early stage plant responses to NP exposure.

KEYWORDS: nanofertilizer, nanoagriculture, micronutrient, bioaccumulation, uptake



INTRODUCTION

Metabolomics is emerging as a very important tool for elucidating the potential benefits and risks of employing nanomaterials (NMs) to enhance agricultural production.¹ It is in the past few years that metabolomics has risen as an important tool in crop production enhancement.^{2–6} Determining the up- or down-regulation of metabolites as a function of NM exposure can serve to evaluate hypotheses regarding the expected improvement in crop yield or unexpected changes in nutritional value, plant health, or other outcomes. One of the major advantages of metabolomics relative to traditional toxicology is that changes in metabolite levels can be detected at lower, more realistic exposure concentrations.

NMs have been proposed for use as nanofertilizers,⁷ nanopesticides,⁸ and even nanosensors.⁹ Compared with conventional agrochemicals, nanofertilizers and nanopesticides may have 20–30% higher efficacy in delivering the target active ingredient (nutrients or pesticides), which could substantially reduce the use of agrochemicals.¹⁰ Molybdenum (Mo) is an essential micronutrient required for the growth of most plants,¹¹ mainly accessible to plants as MoO_4^{2-} .^{7,12–16} Mo usually participates in reductive and oxidative reactions in plants via specific plant enzymes.¹⁴ Mo plays an important role in N fixation in legumes and in regulation in other plants of

nitrate reduction, as well as amino acid and protein biosynthesis.¹¹ Application can be approximately 0.5 kg/ha, requiring careful dosing.¹⁷ While the role of molybdenum in plant growth is indeed significant, studies on the applications of nano- MoO_3 as a micronutrient and/or promotor of plant growth are rather limited.^{1,18–22} Applications at the nanoscale may result in more effective dosing. Thus, studies on the accumulation and uptake of Mo and Mo oxide nanoparticles (NPs) have been conducted on various plant species, such as maize (*Zea mays* Weike720),²³ rice (*Oryza sativa* L.),^{18,22} cowpeas (*Vigna unguiculata*),¹⁹ potato (*Solanum tuberosum* L.),²⁰ and spinach (*Spinacia oleracea* L.).²¹ However, excess Mo NP exposure can inhibit root growth/elongation, prolong seed germination, increase nitrate reductase, and cause oxidative imbalance.^{18–22} While it is useful to study the physiological responses of plants to Mo NPs, a molecular level examination of the effect of Mo NPs is needed. Thus,

Special Issue: Environmental Implications of Nanofertilizers

Received: February 3, 2021

Revised: May 14, 2021

Accepted: May 17, 2021

metabolomics is a useful tool to explore the response of crop plants to Mo NPs.

Metabolites are the end products of cellular regulatory processes; monitoring metabolite changes at the molecular level in plant tissues enhances the information provided by physiological measurements.²³ For example, the physiological data from a study conducted by Olkhovych et al. (2018) showed that Zn NPs resulted in discoloration of *Pistia stratiotes* L. leaves, but this was not the case for Cu NPs.²⁴ In contrast, levels of eight amino acids were significantly altered after Cu NP exposure but only five amino acids were dysregulated after Zn NP exposure.²⁴ Amino acids can act as metal-chelators, signaling molecules, and antioxidant agents during plant defense reactions.²⁵ The changes in amino acid levels illustrate the adaptive ability of plants under environmental stress. Another metabolomics study employed liquid chromatography–mass spectrometry (LC-MS) to analyze changes in polyphenol levels in cucumber leaves exposed to copper.²⁶ Even though leaf biomass remained unchanged for all applied concentrations (i.e., 0.21, 2.1, and 10 mg Cu/plant), the levels of some polyphenol compounds (e.g., *N*-acetyl-L-methionine and *N*-acetyltryptophan) exhibited a significant change even when the copper dose was as low as 0.21 mg Cu/plant. *N*-Acetyl-L-methionine is a superior reactive oxygen species (ROS) scavenger, and *N*-acetyltryptophan can prevent protein molecules from undergoing oxidative degradation.

Metabolomics studies can be untargeted or targeted. Untargeted metabolomics studies serve for a broad, semi-quantitative assessment of the changes in hundreds or thousands of metabolites due to a particular exposure¹ and are useful for generating hypotheses. They are semiquantitative, since standards are not used to accurately quantify the changes in metabolite levels in plant tissues as a function of the exposure to stressors such as NPs. There are several recent untargeted metabolomics studies on the effects of NMs on plants.^{27–34} For example, by studying the metabolic responses of corn (*Zea mays*) leaves to Cu(OH)₂ NPs through leaf exposures, Zhao et al. (2017) discovered that a dose of 100 mg of Cu(OH)₂ NPs per plant significantly increased phenylalanine (23.9%), tyrosine (39.5%), and 4-hydroxycinnamic acid (121.9%).²⁹ Several pathways were perturbed (e.g., glycolysis pathway, tricarboxylic acids cycle (TCA), and shikimate-phenylpropanoid biosynthesis), indicating the activation of energy metabolism and plant defense processes.³⁰ In another study, foliar application of Ag NPs and Ag ions to cucumber (*Cucumis sativus*) leaves indicated that phytol was significantly increased (1.5–2.2-fold) and implicated the degradation of the photosynthesis process.³² In addition, the significant upregulation of antioxidants (arbutin and salicin) and aromatic compounds (4-hydroxyquinazoline, 3-hydroxybenzoic acid, 1,2,4-benzenetriol, and pyrogallol) demonstrated the activation of plant defense systems (i.e., triggered by the overproduction of reactive oxygen species (ROS)). However, due to the semiquantitative nature of the untargeted metabolomics and challenges in detecting less abundant compounds, subtle yet statistically significant changes in metabolite levels may remain hidden.

Targeted metabolomics provide a more rigorous quantitative approach, which can serve to test hypotheses, albeit usually considering a smaller number of metabolites.^{35–39} Calibration with isotopically labeled internal standards is used for absolute quantification of the target metabolites. In addition to calibration curves for each metabolite, the recovery of each

metabolite from the plant tissue is also determined, which is an important factor in the overall analysis. Huang et al. (2018) conducted a systematic study of plant tissue (cucumber leaves) extraction and LC-MS/MS optimization for 23 amino acids.³⁶ The high sensitivity (limit of detection as low as 0.005 ng/mL) and high recovery rates (80–120%) proved the precision and accuracy of targeted analysis. In addition, the levels of many amino acids in cucumber leaf tissues exposed to Cu NPs were significantly altered. In another recent study, targeted metabolomics was employed to study algae exposed to Ag NPs; 94 metabolites were considered, including amino acids, nucleobases/sides/tides, amines, antioxidants, organic acids/phenolics, sugars/sugar alcohols, and fatty acids.³⁸ These metabolites were selected after a preliminary analysis with untargeted metabolomics revealed that these were the most dysregulated. Ag NPs were shown to affect amino acid metabolism, the TCA cycle, and oxidative stress. An analysis of the overall response indicated that 52 metabolites were responsible for the discrimination between control and treatments, and 45 dysregulated metabolites could be identified. Similarly, a targeted metabolomics study of soybean shoots exposed to quantum dots with a similar set of targeted metabolites identified 23 perturbed metabolites in the roots and 26 in the leaves.³⁵ In both cases, the statistical analysis was performed on the entire set of metabolites, to identify the metabolites responsible for the separation between control and treatments, and then characterize the metabolites that are more distinctly dysregulated. Statistical evaluation of all the detected metabolites is the conventional approach in both untargeted and targeted metabolomics. However, the natural concentrations of different groups of metabolites can vary over orders of magnitude, such that the dysregulation (i.e., up-regulated or accumulated or down-regulated or depleted) of much less abundant yet important metabolites may be undetected. We hypothesize that an analysis of the metabolites by groups can reveal more information and add more value than the conventional (overall) analysis.

For this study, corn (*Zea mays* “Golden Bantam”) and wheat (*Triticum spp.* “Red Fife”) were selected, since they are major cereal crops, to study the effect of root exposure to various levels of Mo NPs and the corresponding ionic Mo concentrations. In addition to a targeted metabolomics study, we considered physiological effects, changes in nutrient uptake, and Mo uptake and translocation, to relate the metabolic changes to actual exposure levels. Furthermore, groups of metabolites were also statistically analyzed to extract additional information on dysregulated metabolites. This work provides valuable information on early stage plant responses to Mo NPs at the molecular level and a more comprehensive metabolite data analysis approach for future metabolomics studies.

■ MATERIALS AND METHODS

Characterization and Stability of MoO₃ NPs. MoO₃ NPs were purchased from U.S. Research Nanomaterials, Inc. (US3330), with the primary particle size in a range of 13–80 nm. NP morphology was characterized by transmission electron microscopy (TEM) (FEI Tecnai G2). Surface bonding characteristics of MoO₃ NPs and the phase/crystalline structure were characterized by X-ray photoelectron spectrometry (XPS, Thermo Scientific, ESCALAB 250 XI+) and an X-ray diffraction (XRD) spectrum (Panalytical Empyrean Powder). The hydrodynamic diameter and the surface charge (zeta potential) of MoO₃ NPs in 10% Hoagland water were

measured via dynamic light scattering (Zetasizer Nano ZS, Malvern) at 100 and 500 mg/L levels. Diluted Hoagland water (Table S1) was employed throughout the study to provide sufficient nutrients for plant growth. A molybdenum ionic salt ($\text{Na}_2\text{MoO}_4 \cdot 2\text{H}_2\text{O}$, $\geq 99\%$) was purchased from Sigma-Aldrich, and the concentrations used in the treatments were determined from the stability/dissolution experiments of the MoO_3 NPs as described below.

The suspension stability was evaluated in the 10% Hoagland water solution at 100 and 500 mg/L. Before the stability test, NP suspensions were sonicated for 30 min and distributed into three 50 mL metal-free polypropylene tubes. After 2 min of vigorously vortexing, 2 mL of aliquot was withdrawn at 0, 6, 24, 72, 120, and 168 h time intervals. The suspensions were then placed in Amicon Ultra 3KDa cutoff centrifugal filters (Sigma-Aldrich, UFC800324), centrifuged at 5000 rpm for 20 min, and the acidified solutions were diluted 10 times for further analysis.³⁵ The target metal ion (i.e., Mo) was measured by inductively coupled plasma–mass spectrometry (ICP-MS) (Agilent 7900, Agilent Technologies).

Corn and Wheat Growth and Exposure Conditions.

Corn and wheat were selected for this study, since they are important cereal crops. Before the germination procedure, all seeds were sterilized with 1% sodium hypochlorite solution for 10 min, followed by rinsing 10 times with deionized water. Then the treated seeds were soaked in NANOpure water for another 24 h before germinating in water-saturated vermiculite. Vermiculite was used throughout the study to obtain the desired drainage and avoid accumulation of metals and nutrients. After 7 d, seedlings were transplanted to obtain two wheat seedlings per pot and one corn seedling per pot for the exposure test.

Before transplanting the plants for the root exposure experiments, vermiculite was mixed with predetermined levels of NP suspensions or ionic solutions and then was placed into individual pots. No molybdenum was added to the control group. For the experimental groups, 40 g of vermiculite were mixed with 80 mL of MoO_3 NP suspensions or ionic Mo solution before the plant exposure assay. The MoO_3 NP suspensions, with concentrations of 100 and 500 mg/L, were sonicated for 30 min and mixed with the preweighted vermiculite to reach 200 and 1000 mg of metal (Mo) content per kg of vermiculite. These doses were selected based on literature values¹⁷ for Mo requirements as well as preliminary experiments to determine observable positive effects and excessive dosing. Background concentrations of Mo in agriculture soils generally range from 0.2–5.0 mg/kg;⁴⁰ however, in mining affected soils, the Mo level can reach up to 2903.91 mg/kg.⁴¹ The selected doses in the current study were in the range as moderate and excessive Mo levels, and they were also comparable with other Mo NP toxicity studies on plant species.^{18–20,22} Based on a related study on the dissolution and aggregation of several metal oxide NPs,⁴² including the MoO_3 NPs used in this study, we determined the concentrations for the ionic Mo treatments corresponding to the level of dissolved metal ions expected in the media, 35 and 225 mg/L Mo, to achieve a bioavailable Mo comparable to the NP treatments.

Treated plants were grown under a 16 h photoperiod (light intensity $150 \mu\text{mol} \cdot \text{m}^{-2} \cdot \text{s}^{-1}$) for 3 weeks at 22 °C and a relative humidity of 60%. Plants were watered every day to maintain the vermiculite water content between 70 and 90%. Each exposure condition had a minimum of three replicates.

Metal Content Accumulation and Distribution. Plant roots were rinsed with deionized water to eliminate vermiculite loosely adhered to the roots, followed by 20 min of soaking and rinsing three times with NANOpure water.⁴³ Before freeze-drying, plants were cut and separated into roots, shoots, and leaves, and the length and fresh weight were recorded. The tissues were freeze-dried and stored at -80 °C until needed. For the analysis, freeze-dried tissues were cut into small pieces and placed in 50 mL digestion tubes. Then, 2 mL of plasma pure HNO_3 was added into the tube and the system was heated at 115 °C for 20 min on an SCP Science SigiPREP hot block digestion system. Then 8 mL of H_2O_2 ($\text{HNO}_3:\text{H}_2\text{O}_2 = 1:4$) was added and continued to heat for another 60 min at 115 °C.^{39,44,45} At the end of the digestion process, the digests were diluted to 50 mL with NANOpure water. The acidified solutions were further diluted 10 times prior to analysis via ICP-MS (Agilent 7900, Agilent Technologies). Along with the target metal ions (i.e., Mo), other macro-nutrients (i.e., Ca, K, Mg, and P) and micronutrients (i.e., Cu, Fe, Mn, and Zn) were also quantified via the ICP-MS analysis.

Metabolite Extraction and LC-MS Analysis. After harvesting and processing, another set of plant tissues was cut and separated into roots, shoots, and leaves and then immediately freeze-dried. After freeze-drying, the samples were ground into a fine powder in liquid nitrogen. The samples were stored in 2 mL Eppendorf microcentrifuge tubes in a -80 °C freezer before further analyses. The metabolite extraction process followed previous studies.^{24,35,37} Briefly, weighted 10–20 mg of frozen, finely ground plant tissue was extracted with 1 mL of 80% methanol/2% formic acid in the 2 mL Eppendorf microcentrifuge tubes. The tubes were vortexed at 3000 rpm, sonicated, and centrifuged at 20 000g for 20 min at each step. The supernatant was transferred into vials for detection and quantification of amino acids, antioxidants, fatty acids, nucleobase/side/tides, organic acids/phenolics, and sugar/sugar alcohols using an Agilent 1260 UHPLC binary pump coupled with an Agilent 6470 triple quadrupole mass spectrometer (LC-MS/MS). The 82 selected metabolites were based on previous untargeted and targeted metabolomics studies that indicated that these metabolites can experience significant dysregulation after NP exposure and play important roles in key metabolic pathways.^{26–38} Data were processed with the Agilent MassHunter Workstation Software Quantitative Analysis (V.B.07.01). The detailed sample preparation, instrument settings, and running parameters are listed in the Supporting Information.

Statistical Analysis. One-way analysis of variance (ANOVA) tests followed by a Fisher's least significant difference method were conducted to identify significant changes between control and the various treatments, for each plant species. More specifically, the physiological parameters, mineral nutrient, and metabolite levels were analyzed using SPSS Statistics 22, with the significant threshold (*p*-value) set at 0.05.

The metabolomics statistical analysis was performed using MetaboAnalyst 5.0 (<https://www.metaboanalyst.ca/>). To set features to be more comparable, before the multivariate statistical analysis, the data were normalized by sum and a log transformation. A supervised partial least-squares discriminant analysis (PLS-DA) was conducted to maximize the separation between the control and the experimental groups, which has been widely adopted in the previous similar studies.^{25,37,38} The importance of a given variable was determined by the variable

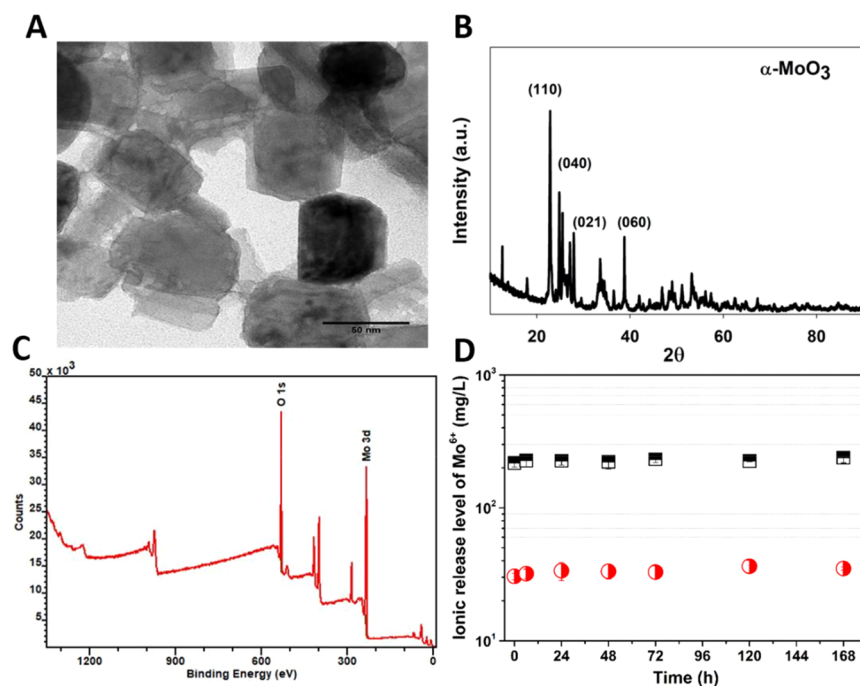


Figure 1. Characterization of MoO₃ NPs. (A) Transmission electron microscope (TEM) imaging, (B) X-ray diffraction (XRD) pattern and *h-k-l* reference peaks, (C) X-ray photoelectron spectroscopy (XPS) spectra, and (D) ions released in 10% HA solution from MoO₃ NPs at (red and white circles) 100 mg/L and (black and white squares) 500 mg/L.

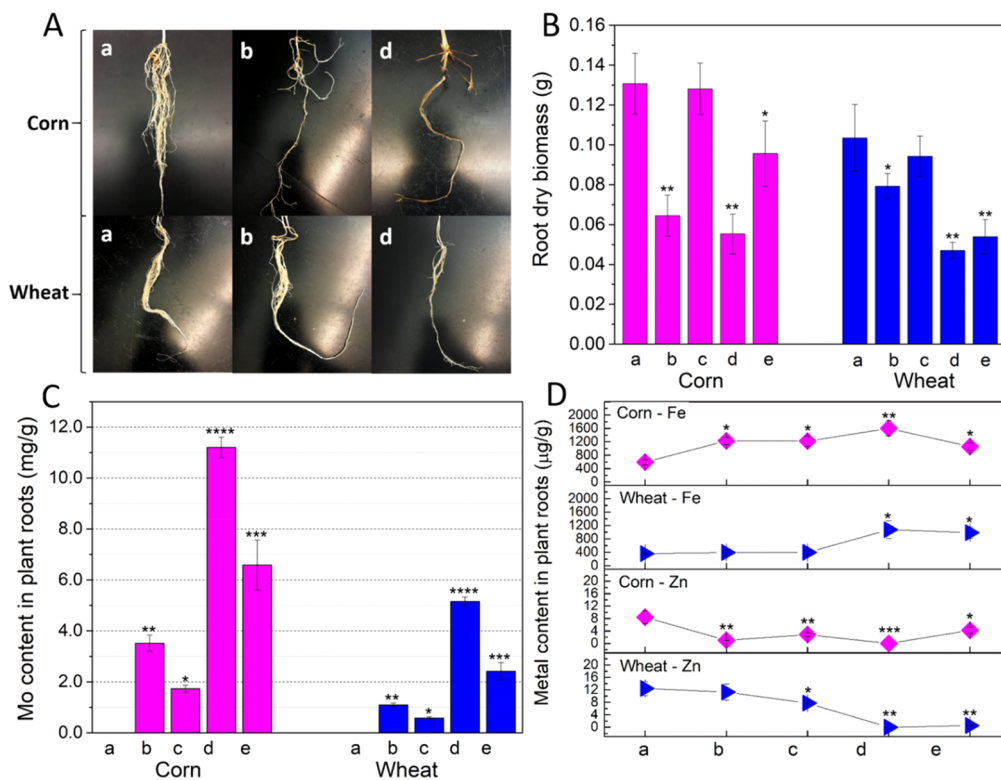


Figure 2. Corn and wheat root responses to MoO₃ NPs and ionic Mo. (A) Images of plant roots after 3 weeks of exposure at different doses; (B) dry biomass of plant roots; (C) Mo content detected in roots; and (D) significantly altered Fe and Zn levels. Treatment conditions: (a) control group (no Mo added), (b) 200 mg of Mo NPs/kg vermiculite, (c) 70 mg of ionic Mo/kg vermiculite, (d) 1000 mg of Mo NPs/kg vermiculite, and (e) 450 mg of ionic Mo/kg vermiculite. Statistics based on a minimum of three replicates. Error bars represent the standard deviation. * indicates significant differences ($p < 0.05$) compared with the control (group a).

importance in projection (VIP), derived from the PLS-DA, considering VIP scores ≥ 1 . The metabolites identified as significant were derived from both the overall and subcategory

metabolites. Metabolite pathway analysis was performed by using MetaboAnalyst 5.0, where the impact value threshold was set at 0.1 for the identification of perturbed pathways.

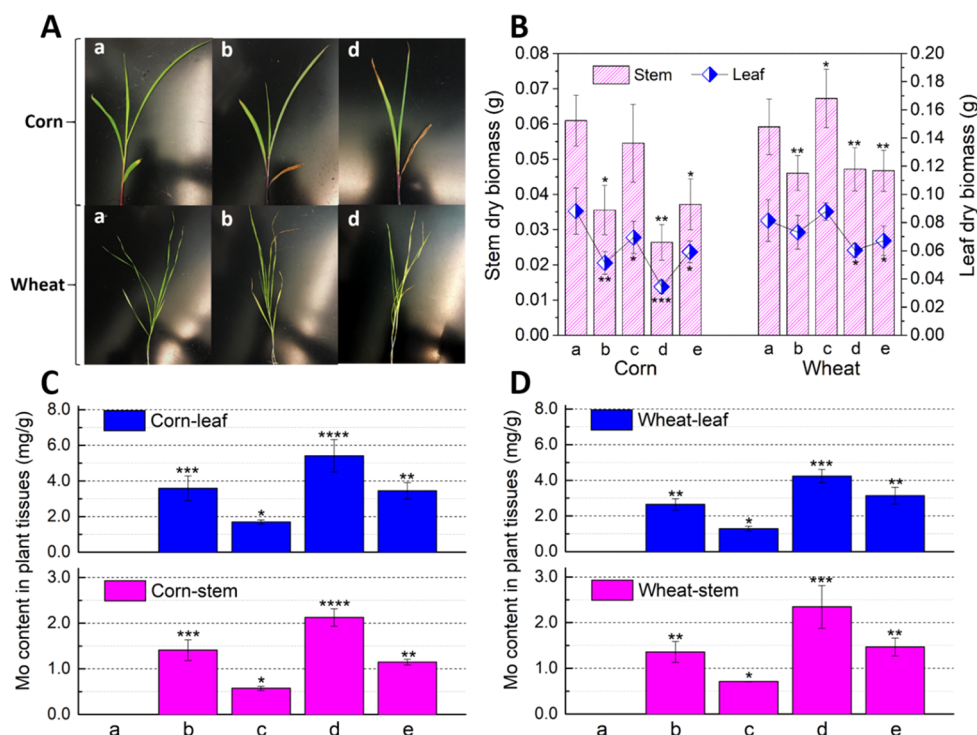


Figure 3. Corn and wheat stem and leaf responses to MoO_3 NPs and ionic Mo. (A) Images of plant stems and leaves after 3 weeks of root exposure at different doses; (B) dry biomass of plant stems and leaves; (C) Mo content in corn tissues; and (D) Mo content in wheat tissues. Treatment conditions: (a) control group (no Mo added), (b) 200 mg of Mo NPs/kg vermiculite, (c) 70 mg of ionic Mo/kg vermiculite, (d) 1000 mg of Mo NPs/kg vermiculite, and (e) 450 mg of ionic Mo/kg vermiculite. Statistics based on a minimum of three replicates. Error bars represent the standard deviation. * indicates significant differences ($p < 0.05$) compared with the control (group a).

RESULTS AND DISCUSSION

Characterization of MoO_3 NPs and the Stability in the Solution.

Both the original MoO_3 NP powder and the nanoparticle suspensions were characterized at the applied conditions (Figure 1). As shown in the TEM image, the original MoO_3 NPs were largely spherical with a diameter 30–60 nm (Figure 1A). The XRD spectra demonstrated that the MoO_3 NPs exhibit an orthorhombic crystalline structure associated with the alpha (α) mineral phase. Furthermore, XPS revealed a primary peak of Mo 3d located at 230.9 eV, indicating Mo was bonded to oxygen in the upper energy levels; no carbon-based coating was detected (Figure 1B,C). For the MoO_3 NP suspensions in 10% Hoagland media at 100 and 500 mg/L, the hydrodynamic diameter ranged from 375.7 ± 18.7 nm to 399.5 ± 7.3 nm and the zeta potentials from -32.0 ± 2.1 to -32.8 ± 1.2 mV, with little difference between NP concentration levels. However, dissolution was a strong function of NP concentration, with a very rapid release of Mo ions even at the beginning of the dissolution test (Figure 1D). At time 0, dissolution (free Mo ion) was 30.5% for the 100 mg/L suspension and 43.5% for the 500 mg/L suspension. Minor changes were observed after 7 days, with an additional 4.5% and 4.1% dissolution for the lower and higher MoO_3 NP levels, respectively. This result was comparable with a recent study where the dissolution rate of 100 mg/L MoO_3 NPs was 35% at time 0 and 39% on day 6 in DI water.⁴² However, when rice seedlings were immersed in a Hoagland water solution, the MoO_3 NP dissolution rate decreased significantly to around 10%.²² Based on the dynamic dissolution behavior of MoO_3 NPs, 35 and 225 mg/L Mo were chosen as the comparable

ionic Mo concentrations corresponding to 100 and 500 mg/L MoO_3 NP suspensions, respectively.

Physiological Response and Metal Accumulation. The root morphology was significantly altered, with inhibited root growth and development of lateral roots, when corn and wheat were exposed via the roots to MoO_3 NPs at 200 mg/kg (treatment b) and 1000 mg/kg (treatment d) compared to the control (treatment a) (Figure 2A). The effect was more pronounced for corn seedlings and at 1000 mg/kg NPs (treatment d). Exposure to the NPs at these concentrations also significantly reduced root dry biomass (Figure 2B), particularly for treatment d with a 58% decrease in root biomass. There was no noticeable effect for treatment c (70 mg/kg ionic Mo), whereas treatment e (450 mg/kg ionic Mo) did result in a significant decrease in root biomass for both corn and wheat. The decrease in root biomass correlated well with Mo content in the roots (Figure 2C), where the control group accumulated less than 0.001 mg Mo/g dry mass, but accumulation increased to 3.5 and 11.2 mg/g in corn roots exposed to 200 and 1000 mg/kg NPs, respectively. The corresponding ionic exposure treatments (c and e) accumulated 1.7 and 6.9 mg/g, which is 47% and 59% of the comparable NP treatments. Wheat accumulated 21.7–68.9% as much Mo as corn, from either the NP exposures or the ionic Mo solutions. As expected, the higher Mo dose resulted in more pronounced changes (Table S2). Uptake of Mo resulted in increased uptake of Fe in corn roots, for all treatments (Figure 2D). For wheat, this only was significant for the high level (1000 mg/kg NPs and 450 mg/kg ionic) treatments. There was a 55% decrease in wheat root biomass for 1000 mg/kg NPs (treatment d). However, uptake of Mo resulted in decreased uptake of Zn in both corn and wheat, for almost all

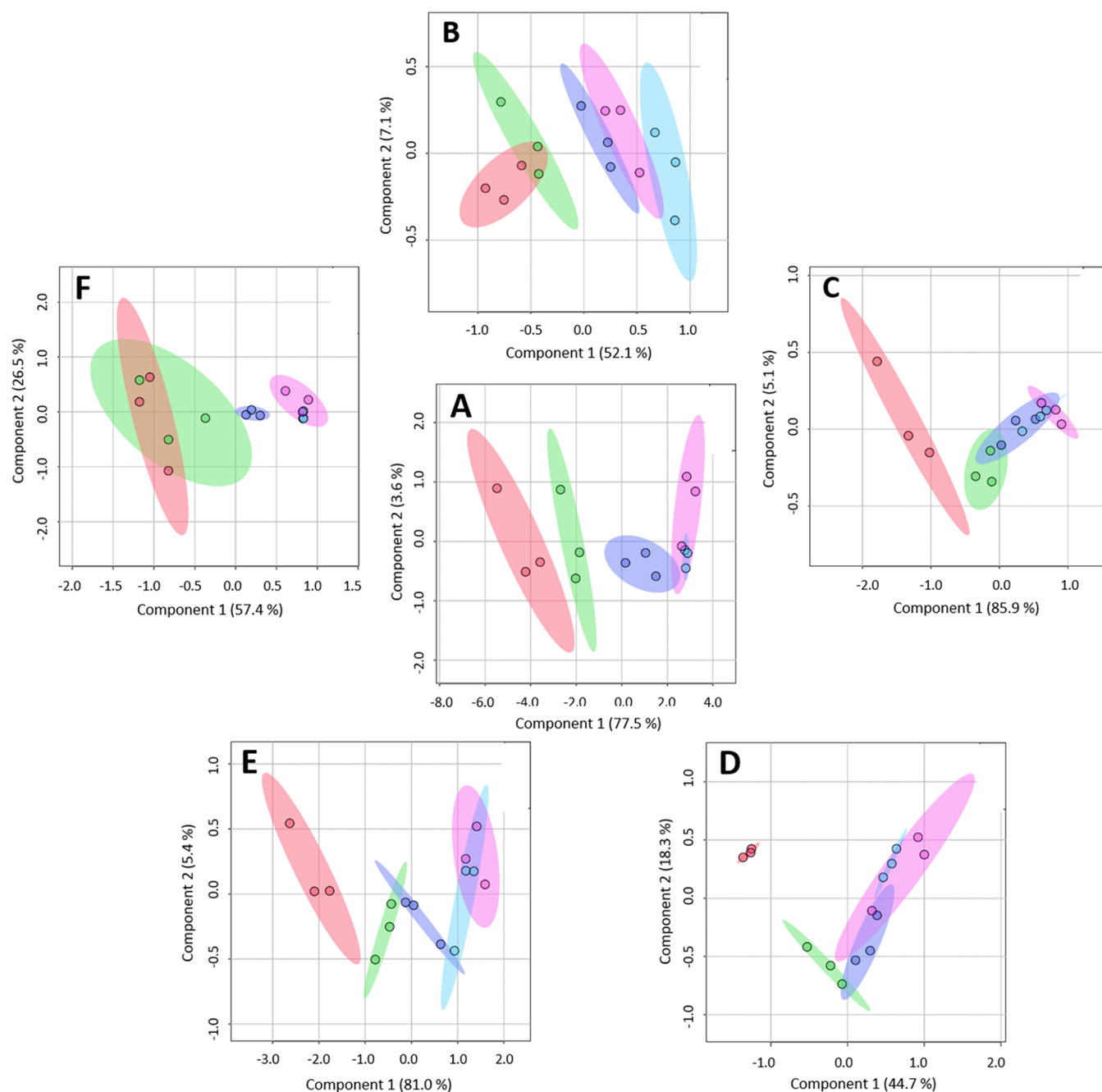


Figure 4. Partial least-squares discriminate analysis (PLS-DA) score plot of (A) the overall, (B) amino acid, (C) antioxidant, (D) nucleic acid, (E) organic acid, and (F) sugar metabolite profiles in corn roots for different root Mo exposures. Symbols (a)–(e) represent different conditions: (a, red circles) control group (no Mo added), (b, green circles) 200 mg/kg MoO_3 NPs, (c, purple circles) 70 mg/kg Na_2MoO_4 , (d, blue circles) 1000 mg/kg MoO_3 NPs, and (e, pink circles) 450 mg/kg Na_2MoO_4 .

treatments, although more pronounced for the high-level treatments. This is an important concern, since lower Zn levels may affect the nutritional value of these crops. Insufficient supply of vitamins and micronutrients (e.g., Zn and Fe) from food commodities (e.g., wheat) affects about two billion people worldwide.⁴⁶

Exposure to Mo via the roots, either as NP or ionic, also affected above ground physiological responses and metal accumulation/translocation (Figure 3). The first true leaves of corn exposed to Mo, particularly at high levels, began to yellow and exhibit signs of senescence; wheat seedlings appeared to be less impacted (Figure 3A). Exposure had a negative effect on

above-ground biomass, with a significant decrease in stem (up to 57%) and leaf biomass (up to 61%) for corn exposed to the 1000 mg/kg NPs (treatment d) and 450 mg/kg ionic (treatment e). The biomasses of wheat stem and leaf were less affected; moreover, there was a statistically significant increase (14%) in stem biomass for the 450 mg/kg ionic (treatment c). There was significant translocation of Mo from the roots to stems and leaves, which was more pronounced for the NP treatments than the corresponding ionic Mo treatments (Figure 3C,D), where 1.6–3.0 times more Mo was translocated to plant leaves than stems. Under the same experimental conditions, corn translocated 1.10–1.36 times

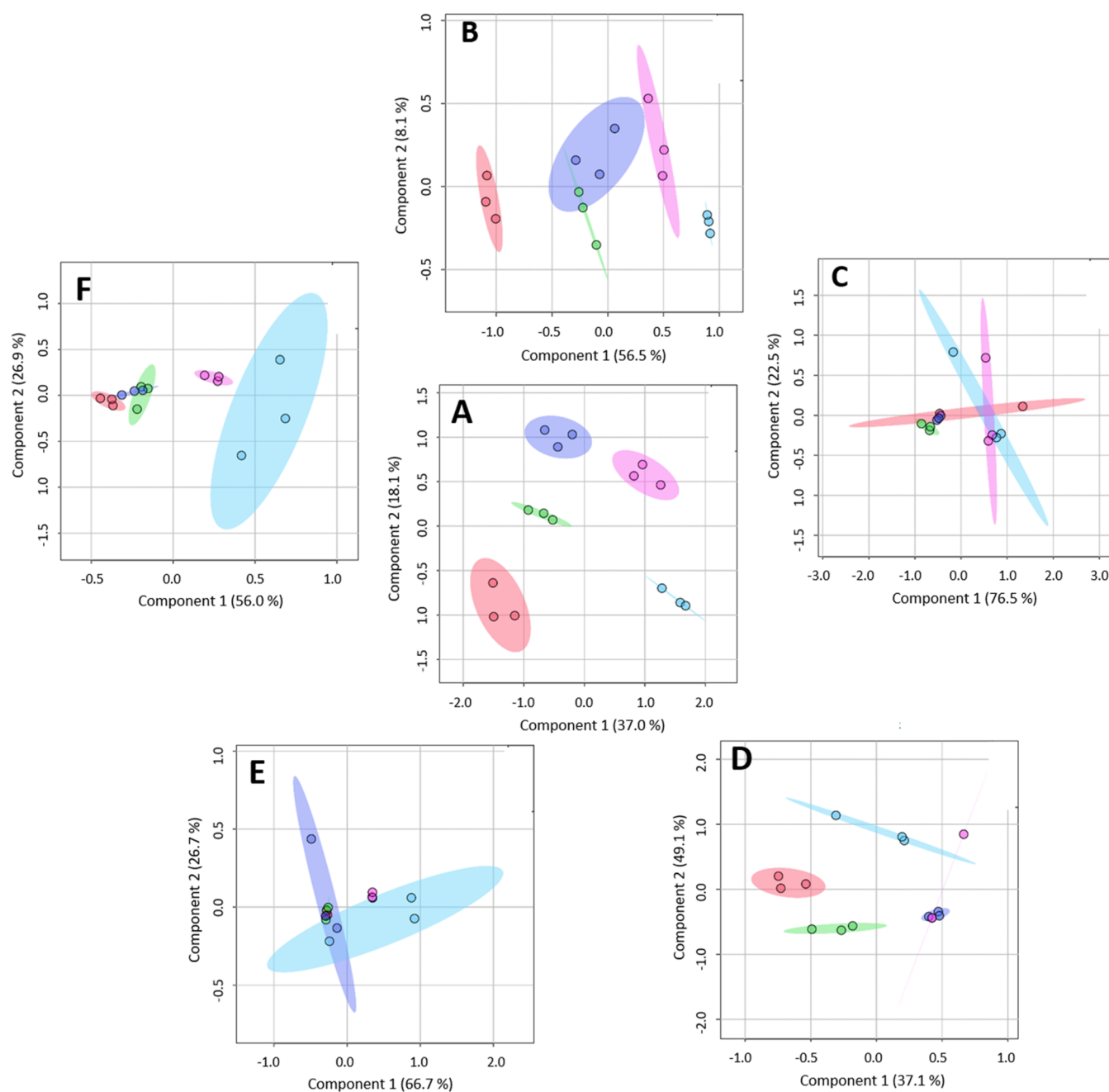


Figure 5. Partial least-squares discriminate analysis (PLS-DA) score plot of the (A) overall, (B) amino acid, (C) antioxidant, (D) nucleic acid, (E) organic acid, and (F) sugar metabolite profiles in wheat roots for different root exposures. Symbols (a)–(e) represent different conditions: (a, red circles) control group (no Mo added), (b, green circles) 200 mg/kg MoO_3 NPs, (c, purple circles) 70 mg/kg Na_2MoO_4 , (d, blue circles) 1000 mg/kg MoO_3 NPs, and (e, pink circles) 450 mg/kg Na_2MoO_4 .

more Mo into leaf tissues than wheat. This result likely explains the earlier leaf morphology alterations observed for corn leaves. Excessive application of nanosized octahedral hexamolybdenum clusters also greatly inhibited rapeseed (*B. napus*) growth.⁴⁴

Root Metabolomics of Corn and Wheat Exposed to MoO_3 NPs and Ionic Mo. Since the plants were exposed via the roots and root tissues accumulated significant amounts of Mo (Figure 2C), the changes in metabolite levels were expected to be most noticeable in these tissues, particularly for corn. The overall PLS-DA analysis of the 82 metabolites clearly indicated separation of the control and the treatments for corn roots (Figure 4A and Figure S1) and for wheat roots (Figure

5A and Figure S1). For corn roots, there was also clear separation for the 200 mg/kg NPs (treatment b) compared to the corresponding 70 mg/kg ionic Mo (treatment c). However, the high-level exposures (treatments d and e) for corn roots overlapped, indicating a similar metabolomics response. In the case of wheat roots, the metabolite profiles separated well among different treatment conditions.

Analysis of individual metabolite groups yielded further insights. Since only one fatty acid was detected in roots (linoleic acid), this group was not analyzed in detail. There was clear separation of antioxidants, nucleic acids, and organic acids between the control and the treatments in corn roots (Figures 4C–E), indicating that, in corn, these groups of

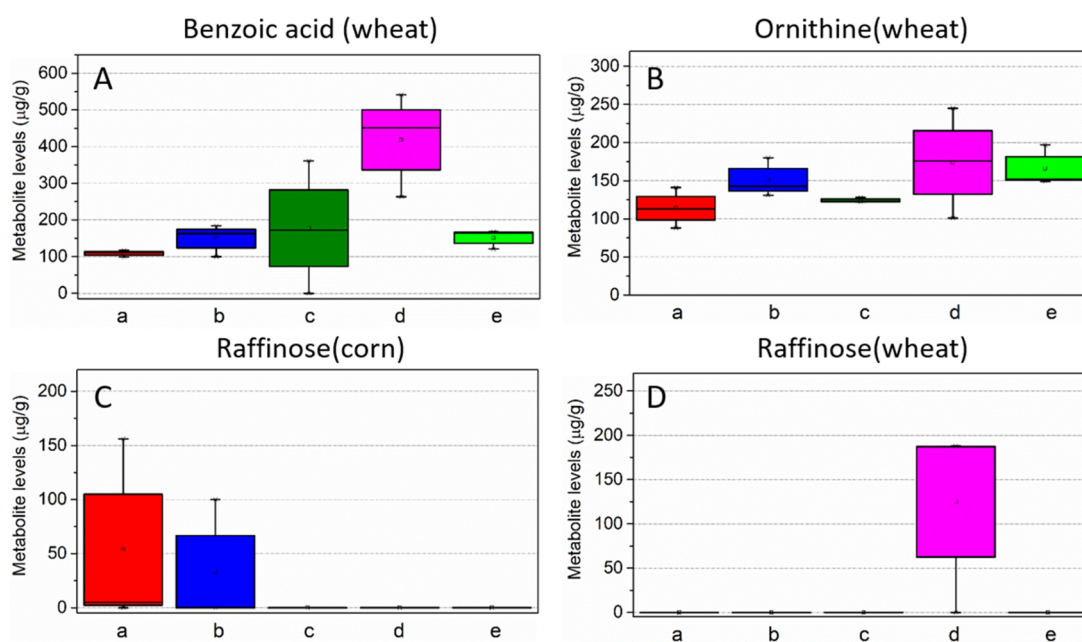


Figure 6. Box plot of metabolites with VIP score > 1 that could only be detected when the individual metabolite categories were analyzed in corn and wheat roots. Treatment conditions: (A) control group (no Mo added), (B) 200 mg Mo NPs/kg vermiculite, (C) 70 mg ionic Mo/kg vermiculite, (D) 1000 mg Mo NPs/kg vermiculite, and (E) 450 mg ionic Mo/kg vermiculite.

metabolites are more sensitive to higher levels of Mo. The levels of amino acids and sugars also respond to Mo treatments in corn roots, except the 200 mg/kg MoO₃ NP (treatment b) (Figure 4B,F). Given that corn exhibited a more marked physiological response to the NP and ionic Mo treatments, it follows that the metabolic response would be generally significant for almost all treatments. For wheat, the separation between control and treatments was clear for amino acids and nucleic acids (Figure 5B,D), but the other groups of metabolites overlapped to some extent with the control, in particular for antioxidants (Figure 5C). There was some separation between treatments for the sugars, more distinctly for the high-level NP and ionic treatments (Figure 5F). The metabolomics responses in roots correlated well with the Mo content in roots, where the higher Mo treatment groups (treatments d and e) had 3.2–4.7 times more accumulated Mo than lower Mo exposure conditions (treatments b and c) and the elevated Mo in plant roots resulting in clearer separations from the control group. From these analyses, we began to infer that a more in-depth analysis could yield more insights.

By combining the statistical analyses (PLS-DA and ANOVA) of the individual metabolite groups, three additional metabolites were identified as significantly dysregulated: benzoic acid, ornithine, and raffinose (Figure 6). Even though these three metabolites were not dysregulated in all root exposure treatments, substantial changes were consistently observed at the high Mo NP dose (treatment d). Heat maps and pathway analyses demonstrated that corn root metabolite profiles exhibited more substantial changes than those of wheat roots (Figures S2–S5). The significant accumulation of citric acid, malic acid, and succinic acid in corn roots (Figure S4) indicated perturbation of the tricarboxylic acid (TCA) pathway, which is the major pathway for energy resources and a key metabolic pathway related to many other important biosynthesis intermediates (e.g., plant hormones and amino acids). Unlike corn roots, the TCA cycle in wheat roots was barely perturbed, except that citric acid was slightly decreased

(0.89 times as the control) when exposed to Mo NPs (Figure S5). There were 15 pathways altered in corn roots versus only 2 pathways significantly changed in wheat roots (Table S3). Ornithine was involved in one of the perturbed pathways (glutathione metabolism) in wheat. It is worth noting that ornithine was overlooked by the overall metabolite analysis but was identified via the individual metabolite group analysis. Even though ornithine is a nonessential amino acid, it participates in the central reactions of the urea cycle (Figure S5).

Leaf Metabolomics of Corn and Wheat Exposed to MoO₃ NPs and Ionic Mo. The PLS-DA analysis of the overall set of metabolites in above-ground plant tissues (i.e., stems and leaves) in general indicated good separation between the control and exposure groups (Figures S6 and S7). Similar to the results of root metabolites, the higher Mo exposures usually led to larger separation with respect to the control. Given that a significant amount of Mo was translocated to plant stems (0.57–2.35 mg/g) and leaves (1.28–5.41 mg/g) (Figure 3C,D), significant metabolic reprogramming was hypothesized. Overall, 33 more metabolites were altered in corn roots (Figure S2) than in corn leaves (Figure 7), showing the more extensive metabolite profile alteration in the direct-contact plant tissue sections. In addition, 21 metabolites were differentially expressed in corn leaves, of which 11 were identified by the overall metabolomics analysis. The additional 10 metabolites (circled in red in Figure 7) were only identified when an analysis by groups of metabolites was conducted. Since these 10 metabolites are generally expressed at much lower concentrations than those identified in the overall metabolomics analysis, their dysregulation was difficult to discern, requiring additional analysis. Among them, glutamine and hypoxanthine were involved in the perturbed purine metabolism and two other metabolites (arginine and ornithine) were important metabolites in the perturbed arginine and proline metabolism pathway (Table S4). Glutamine is the primary product of ammonium assimilation,

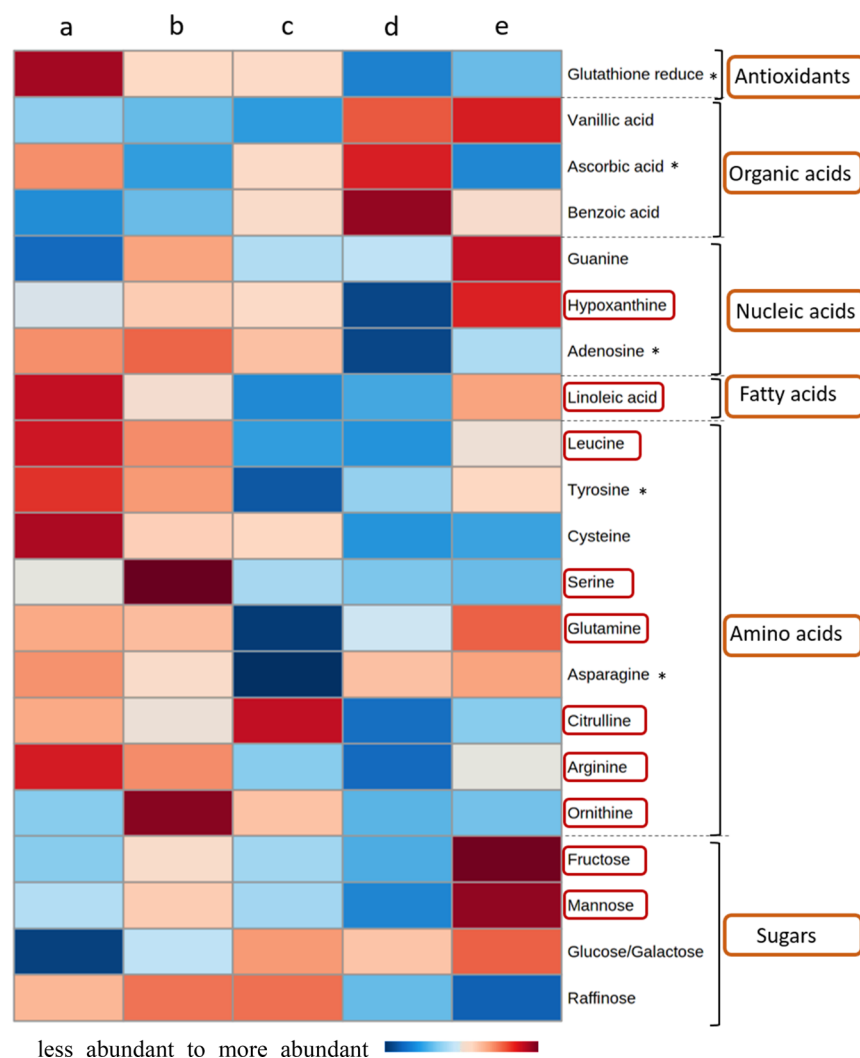


Figure 7. Heat map of corn leaf metabolites with altered levels after root exposure to MoO₃ NPs and ionic Mo. Color bar represents metabolites from less abundant to more abundant. Metabolites circled in red could only be identified when the individual subcategories were analyzed. The asterisk indicates statistically significant differences (p -value < 0.05) in the overall metabolomics analysis. Treatment conditions: (a) control group (no Mo added), (b) 200 mg Mo NPs/kg vermiculite, (c) 70 mg ionic Mo/kg vermiculite, (d) 1000 mg Mo NPs/kg vermiculite, and (e) 450 mg ionic Mo/kg vermiculite.

which is a central metabolite in nitrogen metabolism.⁴⁷ The decreased glutamine levels in corn leaves indicate an altered ability to acquire N compounds. Elevated hypoxanthine, along with other significantly changed metabolites (adenosine and guanine), indicates an alteration of purine metabolism. Arginine serves to store nitrogen in plants, and it is also the signaling molecule in the synthesis of NO, polyamines, and potentially proline.⁴⁸ Even though there are only a few physiological functions where ornithine is presumed to be involved, it is known as a key intermediate for the biosynthesis of arginine, proline, polyamines, glutamate, and alkaloids.⁴⁹

Surprisingly, metabolic reprogramming in wheat leaves exposed to Mo NPs or ions was much more extensive with 53 dysregulated metabolites (Figure 8). Six of the 53 altered metabolites were identified via the deeper analysis, including several nucleic acids and sugars. This was unexpected since all the earlier data (physiological response, changes in biomass, and accumulation of Mo) in wheat leaves indicated less response from wheat leaves than corn leaves. Metabolite pathway analysis revealed that the metabolomic profile was influenced more by Mo NP exposure in wheat leaves than in

corn leaves (Figures S8 and S9). Additional pathways that were perturbed in wheat leaves but not in corn leaves were the TCA cycle, amino acid metabolism, and pyrimidines metabolism. Six metabolites (adenine, adenosine, fructose, asparagine, methionine, tyrosine) had unique responses to exposure to Mo NPs via wheat leaves, and only one metabolite (adenosine) had the same response in corn leaves. It is worth noting that two of the newly discovered metabolites (hypoxanthine and guanosine) from wheat leaves were involved in the significantly perturbed purine metabolism (Figure 8 and Tables S4 and S8). Clearly, there is a level of tolerance for Mo, but at a higher dose it results in substantial metabolic reprogramming.

In summary (Table S5), although clear separation was observed in the overall metabolomics for all treatments vs the control, the separation can be more clearly attributed to different groups of metabolites, with some variation in the response between the two plant species, as well as for the three tissues analyzed (roots, stems, and leaves). The deeper analysis of the metabolomics, going beyond the overall metabolomics to the analysis of the response in individual groups of metabolites, proved useful in identifying additional metabolites

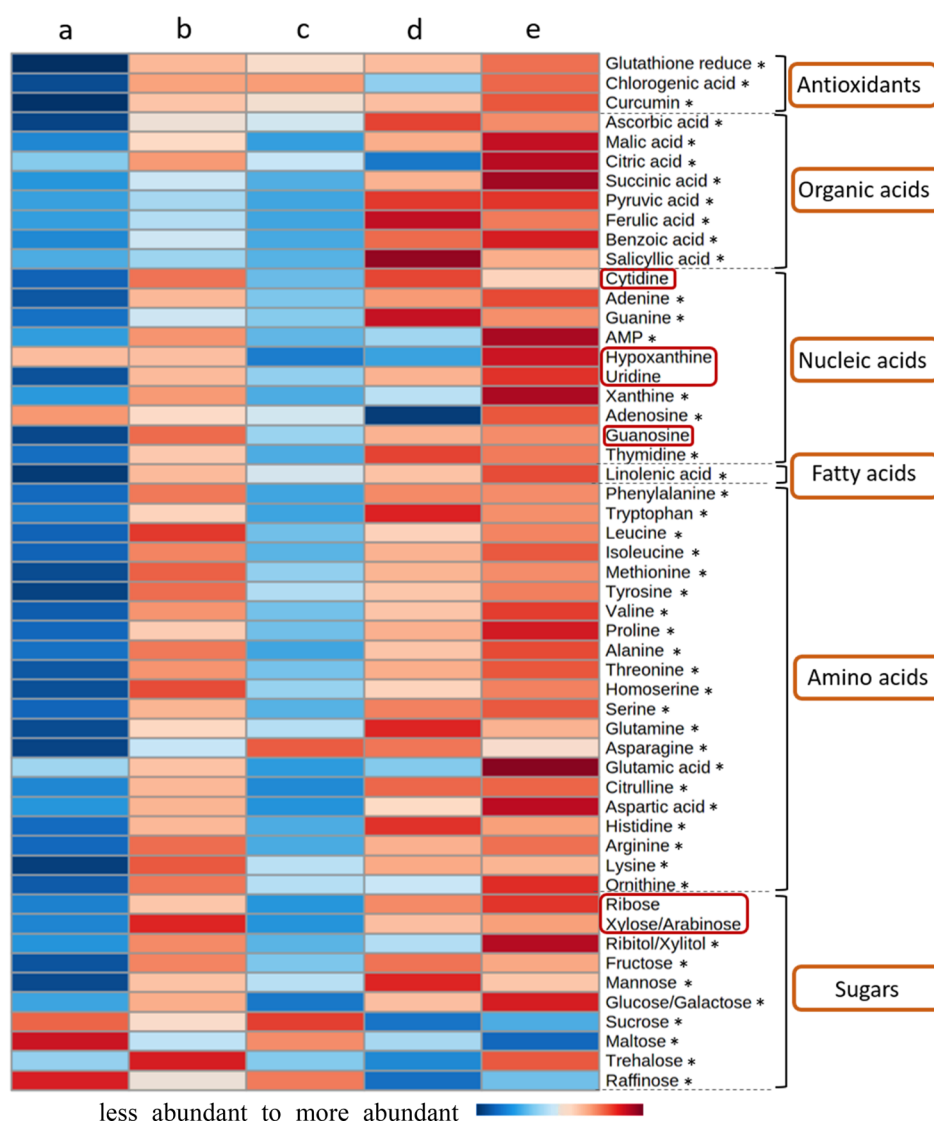


Figure 8. Heat map of wheat leaf metabolites with altered levels after root exposure to MoO₃ NPs and ionic Mo. Color bar represents metabolites from less abundant to more abundant. Metabolites circled in red could only be identified when the individual subcategories were analyzed. The asterisk indicates statistically significant differences (*p*-value < 0.05) in the overall metabolomics analysis. Treatment conditions: (a) control group (no Mo added), (b) 200 mg Mo NPs/kg vermiculite, (c) 70 mg ionic Mo/kg vermiculite, (d) 1000 mg Mo NPs/kg vermiculite, and (e) 450 mg ionic Mo/kg vermiculite.

in plant tissues that responded to Mo root exposures (Figure 9). Summing up the metabolomics analysis of roots, stems, and leaves, seven additional metabolites were discovered that were significantly altered in all plant tissues for corn and also in wheat (Figure 9, Tables S6 and S7). From the individual group analysis, asparagine, fructose, reduced glutathione, and mannose were found as metabolites that were reprogrammed in both corn and wheat plant tissues (from root to leaf). Asparagine (combined with glutamine and arginine) is a major nitrogen transporter and serves to fix N in plants. Thus, changes in asparagine levels may affect the ability of the plant to synthesize N compounds, which could further affect key building blocks of plant proteins and enzymes.⁵⁰ Glutathione plays a crucial role increasing plant tolerance levels and providing efficient protection toward abiotic stress-induced ROS accumulation.⁵¹ Fructose can be produced via glycolysis, and it provides antioxidative properties that promoted plant adaptation to cold weather.⁵² Another simple polysaccharide, mannose, also has been reported to govern the expression of

the antioxidant defense system and to be significantly altered under cold⁵³ and environmental (i.e., SiO₂, TiO₂, and Fe₃O₄) stressors.⁵⁴ These results are comparable to the metabolomics of corn exposed to Cu(OH)₂ NPs,^{30,34} where effects on several metabolic pathways (glycolytic pathway, TCA cycle, and shikimate-phenylpropanoid biosynthesis) and other biosynthetic pathways (e.g., sugars, amino acid, lipids) were observed. However, the key perturbed metabolites were different, indicating that exposure to Mo (NPs and ionic solution) results in very different responses, compared to Cu NPs.

ENVIRONMENTAL SIGNIFICANCE

The metabolomics of two important crops, corn and wheat, were evaluated after exposure to MoO₃ NPs and ionic Mo. The exposures were conducted at two levels, the lower one in the range of a hypothesized beneficial effect and the higher one at a level expected to cause some effects on plant health. Physiologically, corn seedlings were more sensitive than wheat to Mo exposure in general, in either nano- or ionic form,

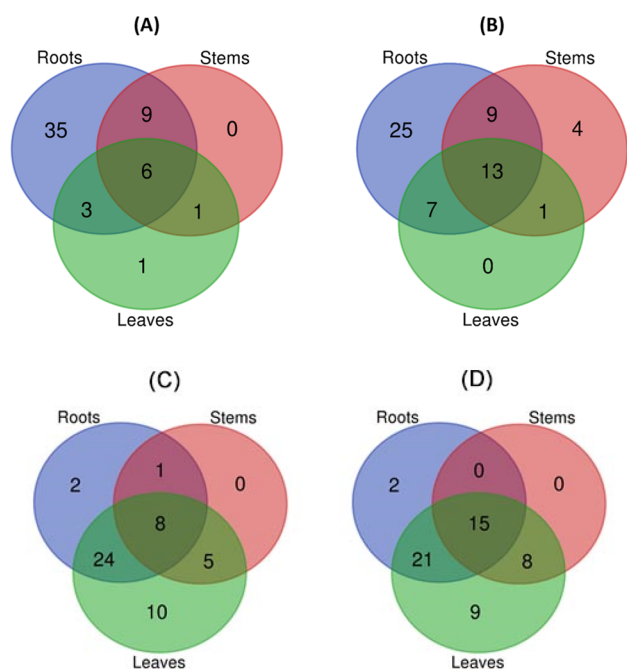


Figure 9. Venn diagram of important metabolites identified in (A) overall corn metabolomics and (B) individual metabolite groups for corn and (C) overall wheat metabolomics and (D) individual metabolite groups for wheat.

exhibiting yellowed leaves and reduced biomass. This likely is a reflection of the higher uptake and translocation of Mo by corn, compared to wheat. Surprisingly, the metabolomics of the wheat exposures to Mo NPs and ions resulted in a dysregulation of more metabolites than corn. In leaves, most of the dysregulated metabolites in wheat exhibited up-regulation, for all Mo treatments. For corn, the pattern of dysregulation was less clear, with both up- and down-regulation of the altered metabolites. There was a clear differential effect between NP and ionic treatments, and plant responses were dose-dependent.

The deeper analysis of the metabolomics, considering different metabolite groups, yielded additional dysregulated metabolites, such as asparagine, fructose, reduced glutathione, and mannose. These results indicate a clear need to understand the benefits of Mo as a nanofertilizer and to tailor the dose at a level that is beneficial for each crop plant, with minimal environmental implications. While this work focused on an early stage crop response to Mo NPs, full life cycle studies are recommended for future work to track the temporal dynamics in metabolite profiles. Additional omics (e.g., genomics, transcriptomics, proteomics) can also be used to further understand the response of plants to nanoagrochemicals and optimize the dose and timing of their application.

■ ASSOCIATED CONTENT

Supporting Information

The Supporting Information is available free of charge at <https://pubs.acs.org/doi/10.1021/acs.est.1c00803>.

Seven tables and nine figures, detailing the growth media, LC-MS/MS methods and analytes, and metabolomics of roots, stems, and leaves, including a pathway analysis (PDF)

■ AUTHOR INFORMATION

Corresponding Author

Arturo A. Keller – Bren School of Environmental Science and Management and Center for Environmental Implications of Nanotechnology, University of California at Santa Barbara, Santa Barbara, California 93106, United States; orcid.org/0000-0002-7638-662X; Phone: +1 805 893 7548; Email: arturokeller@ucsb.edu; Fax: +1 805 893 7612

Authors

Xiangning Huang – Center for Environmental Implications of Nanotechnology, University of California at Santa Barbara, Santa Barbara, California 93106, United States

Pabel Cervantes-Avilés – Escuela de Ingeniería y Ciencias, Tecnológico de Monterrey, Monterrey, Puebla CP 72453, México; Center for Environmental Implications of Nanotechnology, University of California at Santa Barbara, Santa Barbara, California 93106, United States

Weiwei Li – Bren School of Environmental Science and Management, University of California at Santa Barbara, Santa Barbara, California 93106, United States

Complete contact information is available at:

<https://pubs.acs.org/10.1021/acs.est.1c00803>

Notes

The authors declare no competing financial interest.

■ ACKNOWLEDGMENTS

This work was supported by the National Science Foundation (NSF) under cooperative agreement number NSF-1901515. Arturo A. Keller also appreciates Agilent Technologies for their Agilent Thought Leader Award. Pabel Cervantes-Aviles thanks CONACYT. We also thank Dr. Sanghamitra Majumdar for her advice on the experimental approach and Arthur Kao, Devin Everett and Xiaofan Liu for their contributions to the experimental work.

■ REFERENCES

- (1) Majumdar, S.; Keller, A. A. Omics to address the opportunities and challenges of nanotechnology in agriculture. *Crit. Rev. Environ. Sci. Technol.* **2020**, 1–42.
- (2) Johnson, C. H.; Ivanisevic, J.; Siuzdak, G. Metabolomics: Beyond biomarkers and towards mechanisms. *Nat. Rev. Mol. Cell Biol.* **2016**, 17 (7), 451–459.
- (3) Wishart, D. S. Metabolomics for investigating physiological and pathophysiological processes. *Physiol. Rev.* **2019**, 99 (4), 1819–1875.
- (4) Riekeberg, E.; Powers, R. New frontiers in metabolomics: From measurement to insight. *F1000Research* **2017**, 6, 1148.
- (5) Kumar, R.; Bohra, A.; Pandey, A. K.; Pandey, M. K.; Kumar, A. Metabolomics for plant improvement: Status and prospects. *Front. Plant Sci.* **2017**, 8, 1302.
- (6) Sharma, K.; Sarma, S.; Bohra, A.; Mitra, A.; Sharma, N. K.; Kumar, A. Plant Metabolomics: An Emerging Technology for Crop Improvement. *New Vis. in Plant Sci.* **2018**, 65–79.
- (7) Gomez, A.; Narayan, M.; Zhao, L.; Jia, X.; Bernal, R. A.; Lopez-Moreno, M. L.; Peralta-Videa, J. R. Effects of nano-enabled agricultural strategies on food quality: Current knowledge and future research needs. *J. Hazard. Mater.* **2021**, 401, 123385.
- (8) Kah, M.; Hofmann, T. Nanopesticide research: Current trends and future priorities. *Environ. Int.* **2014**, 63, 224–235.
- (9) Giraldo, J. P.; Wu, H.; Newkirk, G. M.; Kruss, S. Nanobiotechnology approaches for engineering smart plant sensors. *Nat. Nanotechnol.* **2019**, 14, 541–553.

- (10) Kah, M.; Kookana, R. S.; Gogos, A.; Bucheli, T. D. A critical evaluation of nanopesticides and nanofertilizers against their conventional analogues. *Nat. Nanotechnol.* **2018**, *13*, 677–684.
- (11) Gupta, U. C.; Srivastava, P. C.; Gupta, S. C. Role of micronutrients: Boron and molybdenum in crops and in human health and nutrition. *Curr. Nutr. Food Sci.* **2011**, *7* (2), 126–136.
- (12) Maillard, A.; Etienne, P.; Diquélou, S.; Trouverie, J.; Billard, V.; Yvin, J.-C.; Ourry, A. Nutrient deficiencies modify the ionic composition of plant tissues: a focus on cross-talk between molybdenum and other nutrients in *Brassica napus*. *J. Exp. Bot.* **2016**, *67* (19), S631–S641.
- (13) Kovács, B.; Puskás-Preszner, A.; Huzsvai, L.; Lévai, L.; Bódi, É. Effect of molybdenum treatment on molybdenum concentration and nitrate reduction in maize seedlings. *Plant Physiol. Biochem.* **2015**, *96*, 38–44.
- (14) Hewitt, E. J.; Bolle-Jones, E. W. Molybdenum as a Plant Nutrient: II. The Effects of Molybdenum Deficiency on Some Horticultural and Agricultural Crop Plants in Sand Culture. *J. Hortic. Sci.* **1952**, *27* (4), 257–265.
- (15) Kaiser, B. N.; Gridley, K. L.; Ngairé Brady, J.; Phillips, T.; Tyerman, S. D. The Role of Molybdenum in Agricultural Plant Production. *Ann. Bot.* **2005**, *96* (5), 745–754.
- (16) Agarwala, S. C.; Sharma, C. P.; Farooq, S.; Chatterjee, C. Effect of molybdenum deficiency on the growth and metabolism of corn plants raised in sand culture. *Can. J. Bot.* **1978**, *56* (16), 1905–1908.
- (17) Reddy, M. M.; Padmaja, B.; Malathi, S.; Rao, L. J. Effects of micronutrients on growth and yield of pigeonpea. *J. SAT Agric. Res.* **2007**, *5* (1).
- (18) Adhikari, T.; Kundu, S.; Rao, A. S. Impact of SiO₂ and Mo Nano Particles on Seed Germination of Rice (*Oryza Sativa* L.). *Int. J. Food Sci. Technol.* **2013**, *4* (9), 809–816.
- (19) Kanneganti, A.; Talasila, M. MoO₃ Nanoparticles: Synthesis, Characterization and Its Hindering Effect on Germination of Vigna Unguiculata Seeds. *J. Eng. Res. Appl.* **2014**, *4* (7), 116–120.
- (20) Mushinskiy, A. A.; Aminova, E. V. Effect of iron, copper and molybdenum nanoparticles on morphometric parameters of *Solanum tuberosum* L. plants. *IOP Conf. Ser. Earth Environ. Sci.* **2019**, *341* (1), 012195.
- (21) Abbasifar, A.; ValizadehKaji, B.; Irvani, M. A. Effect of green synthesized molybdenum nanoparticles on nitrate accumulation and nitrate reductase activity in spinach. *J. Plant Nutr.* **2020**, *43* (1), 13–27.
- (22) Sharma, P. K.; Raghubanshi, A. S.; Shah, K. Examining the uptake and bioaccumulation of molybdenum nanoparticles and their effect on antioxidant activities in growing rice seedlings. *Environ. Sci. Pollut. Res.* **2021**, *28*, 13439–13453.
- (23) Fadeel, B.; Farcas, L.; Hardy, B.; Vázquez-Campos, S.; Hristozov, D.; Marcomini, A.; Lynch, I.; Valsami-Jones, E.; Alenius, H.; Savolainen, K. Advanced tools for the safety assessment of nanomaterials. *Nat. Nanotechnol.* **2018**, *13* (7), 537–543.
- (24) Olkhovych, O.; Volkogon, M.; Taran, N.; Batsmanova, L.; Kravchenko, I. The Effect of Copper And Zinc Nanoparticles on the Growth Parameters, Contents of Ascorbic Acid, and Qualitative Composition of Amino Acids and Acylcarnitines in *Pistia stratiotes* L. (Araceae). *Nanoscale Res. Lett.* **2016**, *11*, 218.
- (25) Hildebrandt, T. M.; Nunes Nesi, A.; Araujo, W. L.; Braun, H.-P. Amino acid catabolism in plants. *Mol. Plant* **2015**, *8* (11), 1563–1579.
- (26) Zhao, L.; Huang, Y.; Paglia, K.; Vaniya, A.; Wancewicz, B.; Keller, A. A. Metabolomics Reveals the Molecular Mechanisms of Copper Induced Cucumber Leaf (*Cucumis sativus*) Senescence. *Environ. Sci. Technol.* **2018**, *52* (12), 7092–7100.
- (27) Zhao, L.; Huang, Y.; Adeleye, A. S.; Keller, A. A. Metabolomics Reveals Cu(OH)₂ Nanopesticide-Activated Anti-oxidative Pathways and Decreased Beneficial Antioxidants in Spinach Leaves. *Environ. Sci. Technol.* **2017**, *51* (17), 10184–10194.
- (28) Zhao, L.; Huang, Y.; Hannah-Bick, C.; Fulton, A. N.; Keller, A. A. Application of metabolomics to assess the impact of Cu(OH)₂ nanopesticide on the nutritional value of lettuce (*Lactuca sativa*): Enhanced Cu intake and reduced antioxidants. *NanoImpact.* **2016**, *3*–4, 58–66.
- (29) Zhao, L.; Hu, Q.; Huang, Y.; Keller, A. A. Response at Genetic, Metabolic, and Physiological Levels of Maize (*Zea mays*) Exposed to a Cu(OH)₂ Nanopesticide. *ACS Sustainable Chem. Eng.* **2017**, *5* (9), 8294–8301.
- (30) Zhao, L.; Huang, Y.; Keller, A. A. Comparative Metabolic Response between Cucumber (*Cucumis sativus*) and Corn (*Zea mays*) to a Cu(OH)₂ Nanopesticide. *J. Agric. Food Chem.* **2018**, *66* (26), 6628–6636.
- (31) Tan, W.; Gao, Q.; Deng, C.; Wang, Y.; Lee, W. Y.; Hernandez-Viezas, J. A.; Peralta-Videa, J. R.; Gardea-Torresdey, J. L. Foliar Exposure of Cu(OH)₂ Nanopesticide to Basil (*Ocimum basilicum*): Variety-Dependent Copper Translocation and Biochemical Responses. *J. Agric. Food Chem.* **2018**, *66* (13), 3358–3366.
- (32) Zhang, H.; Du, W.; Peralta-Videa, J. R.; Gardea-Torresdey, J. L.; White, J. C.; Keller, A.; Guo, H.; Ji, R.; Zhao, L. Metabolomics Reveals How Cucumber (*Cucumis sativus*) Reprograms Metabolites to Cope with Silver Ions and Silver Nanoparticle-Induced Oxidative Stress. *Environ. Sci. Technol.* **2018**, *52* (14), 8016–8026.
- (33) Zhao, L.; Huang, Y.; Hu, J.; Zhou, H.; Adeleye, A. S.; Keller, A. A. 1H NMR and GC-MS Based Metabolomics Reveal Defense and Detoxification Mechanism of Cucumber Plant under Nano-Cu Stress. *Environ. Sci. Technol.* **2016**, *50* (4), 2000–2010.
- (34) Zhao, L.; Huang, Y.; Zhou, H.; Adeleye, A. S.; Wang, H.; Ortiz, C.; Mazer, S. J.; Keller, A. A. GC-TOF-MS based metabolomics and ICP-MS based metallomics of cucumber (*Cucumis sativus*) fruits reveal alteration of metabolites profile and biological pathway disruption induced by nano copper. *Environ. Sci.: Nano* **2016**, *3* (5), 1114–1123.
- (35) Majumdar, S.; Pagano, L.; Wohlschlegel, J. A.; Villani, M.; Zappettini, A.; White, J. C.; Keller, A. A. Proteomic, gene and metabolite characterization reveal the uptake and toxicity mechanisms of cadmium sulfide quantum dots in soybean plants. *Environ. Sci.: Nano* **2019**, *6* (10), 3010–3026.
- (36) Huang, Y.; Li, W.; Minakova, A. S.; Anumol, T.; Keller, A. A. Quantitative analysis of changes in amino acids levels for cucumber (*Cucumis sativus*) exposed to nano copper. *Nano Impact.* **2018**, *12*, 9–17.
- (37) Huang, Y.; Adeleye, A. S.; Zhao, L.; Minakova, A. S.; Anumol, T.; Keller, A. A. Antioxidant response of cucumber (*Cucumis sativus*) exposed to nano copper pesticide: Quantitative determination via LC-MS/MS. *Food Chem.* **2019**, *270*, 47–52.
- (38) Liu, W.; Majumdar, S.; Li, W.; Keller, A. A.; Slaveykova, V. I. Metabolomics for early detection of stress in freshwater alga *Poteroiochromonas malhamensis* exposed to silver nanoparticles. *Sci. Rep.* **2020**, *10* (1), 20563.
- (39) Majumdar, S.; Ma, C.; Villani, M.; Zuverza-Mena, N.; Pagano, L.; Huang, Y.; Zappettini, A.; Keller, A. A.; Marmioli, N.; Dhankher, O. P.; White, J. C. Surface coating determines the response of soybean plants to cadmium sulfide quantum dots. *Nano Impact.* **2019**, *14*, 100151.
- (40) Scheffer, F.; Schachtschabel, P. *Textbook of soil science*; Ferdinand Enke: 1982.
- (41) Shi, Z.; Zhang, J.; Wang, F.; Li, K.; Yuan, W.; Liu, J. Arbuscular mycorrhizal inoculation increases molybdenum accumulation but decreases molybdenum toxicity in maize plants grown in polluted soil. *RSC Adv.* **2018**, *8* (65), 37069–37076.
- (42) Cervantes-Avilés, P.; Huang, X.; Keller, A. A. Dissolution and Aggregation of Metal Oxide Nanoparticles in Root Exudates and Soil Leachate: Implications for Nanoagrochemical Application. *Environ. Sci. Technol.* **2021**, DOI: 10.1021/acs.est.1c00767.
- (43) Hong, J.; Peralta-Videa, J. R.; Rico, C.; Sahi, S.; Viveros, M. N.; Bartonjo, J.; Zhao, L.; Gardea-Torresdey, J. L. Evidence of translocation and physiological impacts of foliar applied CeO₂ nanoparticles on cucumber (*Cucumis sativus*) plants. *Environ. Sci. Technol.* **2014**, *48* (8), 4376–4385.
- (44) Zhao, L.; Hu, Q.; Huang, Y.; Fulton, A. N.; Hannah-Bick, C.; Adeleye, A. S.; Keller, A. A. Activation of antioxidant and

detoxification gene expression in cucumber plants exposed to a Cu(OH)₂ nanopesticide. *Environ. Sci.: Nano* **2017**, *4* (8), 1750–1760.

(45) Aubert, T.; Burel, A.; Esnault, M.-A.; Cordier, S.; Grasset, F.; Cabello-Hurtado, F. Root uptake and phytotoxicity of nanosized molybdenum octahedral clusters. *J. Hazard. Mater.* **2012**, *219*, 111–118.

(46) Müller, C.; Elliott, J.; Levermann, A. Fertilizing hidden hunger. *Nat. Clim. Change* **2014**, *4* (7), 540–541.

(47) Chellamuthu, V.-R.; Ermilova, E.; Lapina, T.; Lüddecke, J.; Minaeva, E.; Herrmann, C.; Hartmann, M. D.; Forchhammer, K. A widespread glutamine-sensing mechanism in the plant kingdom. *Cell* **2014**, *159* (5), 1188–1199.

(48) Winter, G.; Todd, C. D.; Trovato, M.; Forlani, G.; Funck, D. Physiological implications of arginine metabolism in plants. *Front. Plant Sci.* **2015**, *6*, 534.

(49) Majumdar, R.; Minocha, R.; Minocha, S. Ornithine: at the crossroads of multiple paths to amino acids and polyamines. In *Amino acids in higher plants*; D'Mello, J. P. F., Ed.; CABI: Oxfordshire, U.K., 2015; Chapter 9, pp 156–176.

(50) Lea, P. J.; Sodek, L.; Parry, M. A.; Shewry, P. R.; Halford, N. G. Asparagine in plants. *Ann. Appl. Biol.* **2007**, *150* (1), 1–26.

(51) Gallé, A.; Czékus, Z.; Bela, K.; Horváth, E.; Ördög, A.; Csiszár, J.; Poór, P. Plant glutathione transferases and light. *Front. Plant Sci.* **2019**, *9*, 1944.

(52) Bogdanović, J.; Mojović, M.; Milosavić, N.; Mitrović, A.; Vučinić, Z.; Spasojević, I. Role of fructose in the adaptation of plants to cold-induced oxidative stress. *Eur. Biophys. J.* **2008**, *37* (7), 1241–1246.

(53) Chai, F.; Liu, W.; Xiang, Y.; Meng, X.; Sun, X.; Cheng, C.; Liu, G.; Duan, L.; Xin, H.; Li, S. Comparative metabolic profiling of *Vitis amurensis* and *Vitis vinifera* during cold acclimation. *Hortic. Res.* **2019**, *6*, 8.

(54) Zhao, L.; Zhang, H.; White, J. C.; Chen, X.; Li, H.; Qu, X.; Ji, R. Metabolomics reveals that engineered nanomaterial exposure in soil alters both soil rhizosphere metabolite profiles and maize metabolic pathways. *Environ. Sci.: Nano* **2019**, *6* (6), 1716–1727.